AMERICAN SOCIETY FOR MICROBIOLOGY | Antimicrobial Agents and Chemotherapy

In Vitro Assessment of Combinations of Enterovirus Inhibitors against Enterovirus 71

Yizhuo Wang,[a] Guiming Li,[a,b] Shilin Yuan,[a] Qianqian Gao,[a] Ke Lan,[a] Ralf Altmeyer,[c] Gang Zou[a]

Pathogen Diagnostic Center, Key Laboratory of Molecular Virology and Immunology, Institut Pasteur of Shanghai, Chinese Academy of Sciences, Shanghai, China[a]; School of Life Sciences, Shanghai University, Shanghai, China[b]; Shandong University-Helmholtz Institute of Biotechnology, Shandong University, Qingdao, China[c]

Enterovirus 71 (EV-A71) is a major causative pathogen of hand, foot, and mouth disease (HFMD) epidemics. No antiviral therapies are currently available for treating EV-A71 infections. Here, we selected five reported enterovirus inhibitors (suramin, itraconazole [ITZ], GW5074, rupintrivir, and favipiravir) with different mechanisms of action to test their abilities to inhibit EV-A71 replication alone and in combination. All selected compounds have anti-EV-A71 activities in cell culture. The combination of rupintrivir and ITZ or favipiravir was synergistic, while the combination of rupintrivir and suramin was additive. The combination of suramin and favipiravir exerted a strong synergistic antiviral effect. The observed synergy was not due to cytotoxicity, as there was no significant increase in cytotoxicity when compounds were used in combinations at the tested doses. To investigate the potential inhibitory mechanism of favipiravir against enterovirus, two favipiravir-resistant EV-A71 variants were independently selected, and both of them carried an S121N mutation in the finger subdomain of the 3D polymerase. Reverse engineering of this 3D S121N mutation into an infectious clone of EV-A71 confirmed the resistant phenotype. Moreover, viruses resistant to ITZ or favipiravir remained susceptible to other inhibitors. Most notably, combined with ITZ, rupintrivir prevented the development of ITZ-resistant variants. Taken together, these results provide a rational basis for the design of combination regimens for use in the treatment of EV-A71 infections.

Hand, foot, and mouth disease (HFMD) is a common infectious disease caused by enteroviruses that mainly affects children younger than 5 years old. The clinical presentations are usually mild and include fever, skin eruptions on the hands and feet, and vesicles in the mouth. However, a small proportion of affected children may develop neurological and systemic complications such as encephalitis, aseptic meningitis, acute flaccid paralysis, pulmonary edema, cardiopulmonary dysfunction, and even death (1–3). Enterovirus 71 (EV-A71) and coxsackievirus A16 (CV-A16) are the two major causative agents of HFMD. In particular, EV-A71 is often associated with neurological complications and is responsible for the majority of fatalities (4–6). There has been a significant increase in EV-A71 epidemic activity across the Asia-Pacific region since 1997 (7–12). Unfortunately, no approved antiviral therapeutics are currently available for the treatment of EV-A71 infection, and treatment remains limited to supportive care. Although two inactivated monovalent EV-A71 vaccines, manufactured by the Institute of Medical Biology, Chinese Academy of Medical Sciences, and Sinovac Biotech Co., Ltd., were recently approved by the China Food and Drug Administration (CFDA), the vaccines are not free, and residents can choose whether they want to be inoculated. Therefore, anti-EV-A71 drugs are still needed for the treatment of infected individuals whose parents opt not to vaccinate their children.

EV-A71 belongs to the genus *Enterovirus* in the family *Picornaviridae*. The viral genome is a single-stranded, positive-sense RNA of ~7,500 nucleotides. The genomic RNA contains a 5′ nontranslated regions (NTR), a single open reading frame, and a 3′ NTR. The single open reading frame encodes a polyprotein precursor that is processed by viral proteases into four structural proteins (VP4, VP2, VP3, and VP1) and seven nonstructural proteins (2A, 2B, 2C, 3A, 3B [VPg], 3C, and 3D) (13). Drug discovery efforts for new antivirals have focused mainly on two viral proteins, the capsid protein VP1 and the 3C protease (14). The EV-A71 replication cycle involves a number of critical steps, including virus adsorption, uncoating, RNA translation, polyprotein processing, viral RNA replication, and particle assembly. Several key steps in the replication cycle have been identified as valuable targets.

To date, many small molecules have been reported to have inhibitory effects against enteroviruses, particularly rhinovirus, coxsackievirus B3 (CV-B3), and EV-A71. Several compounds have progressed into clinical trials, but none of them has been formally approved by the FDA due to limited efficacy or safety concerns (14–17). Combining antiviral agents with additive or synergistic antiviral effects is a proven strategy to increase antiviral potency and reduce potential toxicity and adverse effects. The success of combination therapy has been exemplified by the treatment of HIV and hepatitis C virus (HCV) infections.

In this study, we used two-drug combination experiments to evaluate the *in vitro* efficacy of combinations of five reported enterovirus inhibitors, including suramin, itraconazole (ITZ), GW5074, rupintrivir, and favipiravir. These inhibitors have distinct mechanisms of action and different resistance profiles. Suramin and its analog NF449 blocked EV-A71 infection at the step of virus binding (18–21), and NF449-resistant viruses contain two mutations (E98Q and K244R) in the VP1 protein (21, 22). ITZ exhibited broad-spectrum antienterovirus activity by target-

Received 22 May 2016 **Returned for modification** 13 June 2016
Accepted 19 June 2016

Accepted manuscript posted online 27 June 2016

Citation Wang Y, Li G, Yuan S, Gao Q, Lan K, Altmeyer R, Zou G. 2016. *In vitro* assessment of combinations of enterovirus inhibitors against enterovirus 71. Antimicrob Agents Chemother 60:5357–5367. doi:10.1128/AAC.01073-16.

Address correspondence to Ralf Altmeyer, altmeyer@sdu.edu.cn, or Gang Zou, gangzou@ips.ac.cn.

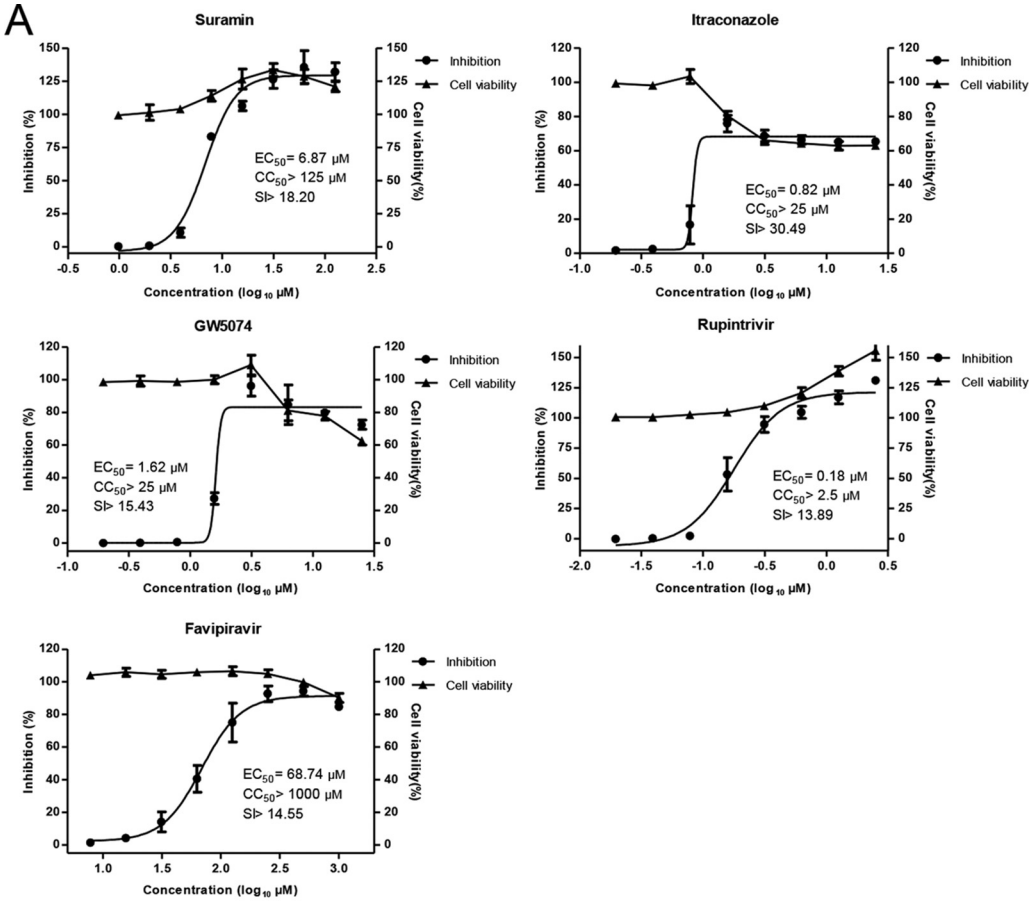
A
Suramin
Inhibition (%)
Cell viability(%)
Inhibition
Cell viability
EC50= 6.87 μM
CC50> 125 μM
SI> 18.20
Concentration (log10 μM)
Itraconazole
EC50= 0.82 μM
CC50> 25 μM
SI> 30.49
GW5074
EC50= 1.62 μM
CC50> 25 μM
SI> 15.43
Rupintrivir
EC50= 0.18 μM
CC50> 2.5 μM
SI> 13.89
Favipiravir
EC50= 68.74 μM
CC50> 1000 μM
SI> 14.55

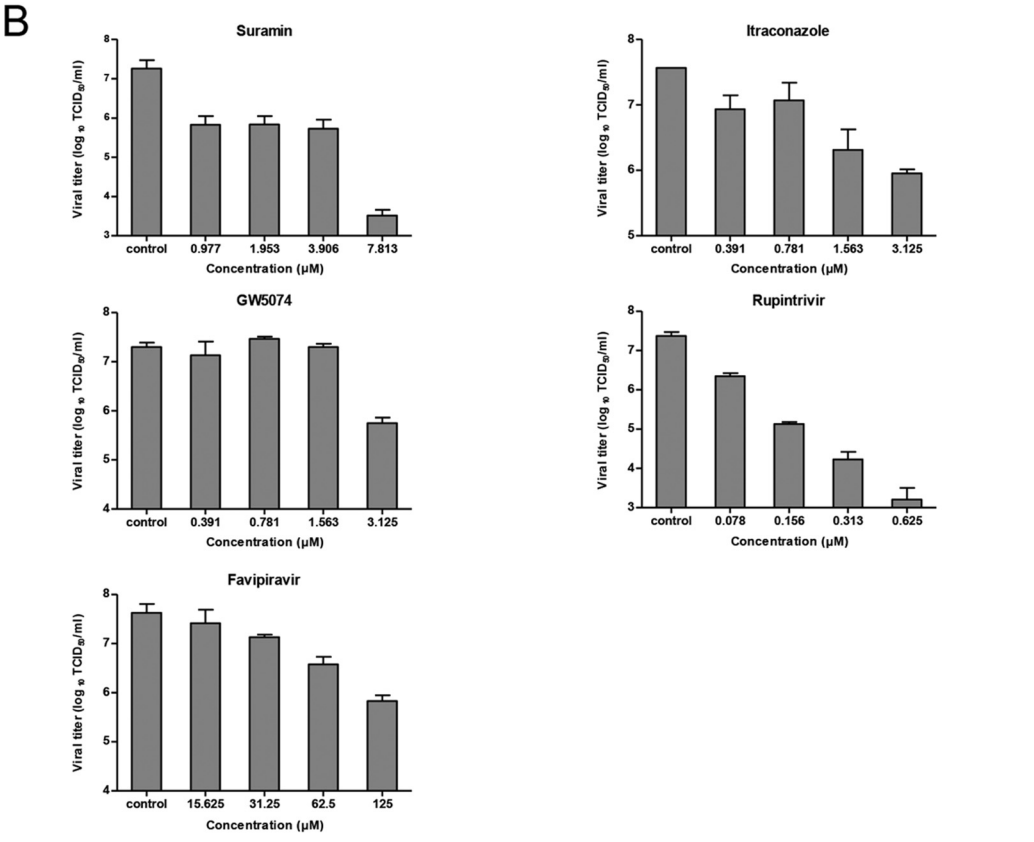
B
Suramin
Viral titer (log10 TCID50/ml)
control
0.977
1.953
3.906
7.813
Concentration (μM)
Itraconazole
0.391
0.781
1.563
3.125
GW5074
Rupintrivir
0.078
0.156
0.313
0.625
Favipiravir
15.625
31.25
62.5
125

ing host oxysterol-binding protein (OSBP) (23), and ITZ-resistant EV-A71 contains a single mutation in the 3A protein (V51L or V75A) (24). GW5074, a Raf-1 inhibitor, exhibited antiviral activity against poliovirus (PV) and EV-A71 (21) by targeting cellular phosphatidylinositol 4-kinase III beta (PI4KB) (25). Enviroxime resistance mutations in PV 3A (A70T) and CV-B3 3A (V45A and H57Y) conferred cross-resistance to GW5074 (26, 27). However, ITZ-resistant EV-A71 did not exhibit cross-resistance to GW5074 (24). Rupintrivir (also known as AG7088), an irreversible inhibitor of the 3C protease, exhibited broad-spectrum antiviral activity against members of the family *Picornaviridae* (28–30), and resistance to rupintrivir was mapped to the V104I mutation in the 3C protease of enterovirus D68 (EV-D68) (31). Favipiravir (also known as T-705) was initially developed as an inhibitor of influenza virus (32) but was later found to inhibit a number of unrelated RNA viruses, including alphaviruses (33, 34), arenaviruses (35, 36), bunyaviruses (35), noroviruses (37), filoviruses (38), flaviviruses (39), and enterovirus (31, 32). Favipiravir inhibits influenza virus in its nucleoside triphosphate form by directly interacting with viral RNA polymerase (40, 41). Selection of favipiravir-resistant variants has been achieved only for chikungunya virus so far (34). To understand the mechanism of action of favipiravir against enterovirus, we generated favipiravir-resistant EV-A71 variants and found that the S121N single mutation in the 3D polymerase was able to confer resistance. Our results showed that three combinations (rupintrivir plus ITZ, rupintrivir plus favipiravir, and suramin plus favipiravir) exerted strong synergistic antiviral effects. These findings provide important insight into the molecular mechanism by which favipiravir exerts its antiviral activity against enterovirus and useful information for the design of combination regimens for future anti-EV-A71 therapies.

MATERIALS AND METHODS

Cells, viruses, and compounds. RD (human rhabdomyosarcoma) cells and Vero (African green monkey kidney) cells were cultured in Dulbecco modified Eagle medium (DMEM; Invitrogen) with 10% fetal bovine serum (FBS) (HyClone; Thermo Scientific) and 100 U/ml penicillin-streptomycin (PS; Invitrogen) at 37°C with 5% CO_2. EV-A71 strain FY573 (GenBank accession no. HM064456) was used for antiviral activity assays and combination studies. EV-A71 strain G082, derived from an infectious cDNA clone, was used for resistance analysis (24). The compounds ITZ, GW5074 (Sigma), rupintrivir (Santa Cruz), and favipiravir (Chembest) were dissolved in dimethyl sulfoxide (DMSO), and suramin (Sigma) was dissolved in DMEM for antiviral experiments.

Cytopathic effect assay and cytotoxicity assay. To test the antiviral activity of individual compounds, a cytopathic effect (CPE) inhibition assay was performed as previously described, with minor modifications (24). Briefly, RD cells (10,000 cells in 50 μl of DMEM) were seeded into each well of a white 96-well plate (Costar; Corning) and incubated at 37°C with 5% CO_2 for 24 h prior to infection. Five microliters of 2-fold serial dilutions of each compound was added to cells. In cell control and virus control wells, 0.25% DMSO or medium was added. Within 10 min of the addition of the compound, 45 μl of diluted virus (150 PFU, which corresponds to a multiplicity of infection [MOI] of 0.015) was added to each well. After 96 h of incubation at 37°C with 5% CO_2, the CPE was measured by using CellTiter-Glo reagent (Promega) with a Veritas microplate luminometer (Turner BioSystems). To control assay quality, the signal-to-background (S/B) ratio and Z factor for each plate were calculated as described previously (24), and plates with an S/B ratio of >10 and a Z-factor value of >0.5 were used for data analysis. The 50% effective concentration (EC_{50}) was defined as the concentration needed to achieve 50% of the maximal inhibition effect. The cytotoxicity of each compound was assessed in parallel by using the same assay without the addition of virus in order to determine the concentration that resulted in 50% inhibition of cell viability (CC_{50}). The selectivity index (SI) was calculated for each compound as SI = CC_{50}/EC_{50}.

Virus yield reduction assay, $TCID_{50}$ assay, plaque assay, and growth curves. RD cells were seeded into 12-well plates at 3×10^5 cells per well in 1 ml of DMEM supplemented with 10% FBS and 100 U/ml PS and incubated at 37°C with 5% CO_2. After 24 h, medium was removed, and cells were infected with EV-A71 strain FY573 at an MOI of 0.1. Compounds were then added to the cell culture media. Plates were incubated at 37°C. After 48 h, the culture media were collected and then subjected to virus titration by a 50% tissue culture infective dose ($TCID_{50}$) assay as described previously (24). For EV-A71 strain G082 and recombinant viruses derived from infectious cDNA clones, Vero cells were used for infection and plaque assays, and other conditions remained unchanged. Plaque assays (24) and growth curves (42) were performed as described previously.

Generation and characterization of favipiravir-resistant EV-A71. Favipiravir-resistant EV-A71 was generated by passaging EV-A71 strain G082 on Vero cells in the presence of favipiravir. For each round of passaging, Vero cells (3×10^5 cells per well) in 12-well plates were infected with 100 μl of EV-A71 (derived from the previous passaging, the first round of infection at an MOI of 0.1) in the presence of increasing concentrations of favipiravir. Three independent selections were carried out in parallel. The initial concentration of favipiravir was 75 μM (~3× the EC_{50} for the virus [strain G082] yield reduction assay on Vero cells), and the concentration was doubled at passage 4 (P4), P7, and P15. (See Fig. 2A for an outline of the strategy used for this selection.) For each passage, viral supernatants were harvested when cells showed apparent CPE. Resistance was determined by the fold change in viral titers between wild-type (WT) and favipiravir-treated viruses at 600 μM favipiravir. The selections were terminated at P16, when no further improvement of resistance was observed. Viral RNAs from passage 16 were extracted from the culture supernatants by using a QIAamp viral RNA minikit (Qiagen). The RNAs were subjected to amplification using SuperScript III one-step reverse transcription-PCR (RT-PCR) kits (Invitrogen). The gel-purified RT-PCR products were subjected to DNA sequencing for the whole genome.

Construction and analysis of an EV-A71 mutant. An EV-A71 genome-length cDNA clone with a specific mutation was constructed by using an infectious cDNA clone, pFLEV71. The methods for mutagenesis of the cDNA clone, *in vitro* transcription, and RNA transfection were reported previously (24). The viruses in the culture fluids were collected every 24 h until an apparent CPE was observed from 24 h posttransfection. Aliquots of the viruses were stored at −80°C. Viral titers were determined by a plaque assay on Vero cells.

Combination studies. The antiviral effects of the drug combinations on EV-A71 replication were determined by a CPE assay as described

FIG 1 Antiviral activities of individual compounds against EV-A71. (A) Antiviral activities and cytotoxicities of individual compounds. Twofold serial dilutions of compounds were added to RD cells, and the inhibitory effects of the compounds were analyzed by a CPE assay. EC_{50}s were calculated by using Prism nonlinear regression (GraphPadPrism5). Cytotoxicity was also examined by incubation of RD cells with the indicated concentrations of compounds. Cell viability was measured by using CellTiter-Glo reagent and is presented as the percent luminescence derived from the compound-treated cells compared to that from the mock-treated cells. (B) Antiviral effect of selected compounds on virus yield. RD cells were infected with EV-A71 strain FY573 at an MOI of 0.1 and treated with 2-fold serial dilutions of compounds. Supernatants were collected at 48 h postinfection, and viral titers were determined by a $TCID_{50}$ assay. The data shown were obtained from two independent replicates. Error bars indicate the standard deviations from two independent experiments.

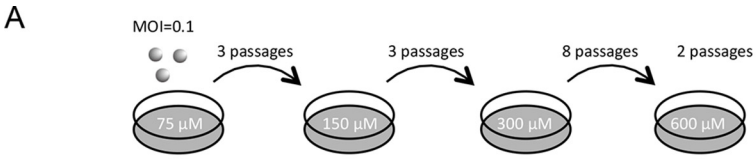

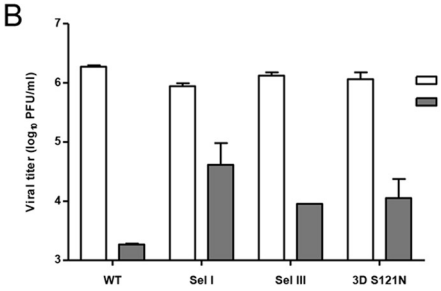

Virus	Fold reduction	Fold change
WT	1013.5	1.0
Sel I	21.2	47.8
Sel III	147.2	6.9
3D S121N	102.2	9.9

C

Selections	Nucleotide and Amino acid substitution(s) within:				
	VP2	VP1	2B	2C	3D
Sel I	A1394G, M149V	A2792C, M119L	A3941G, I55V	T4925C, L284L	A6221G, S96G G6297A, S121N A6428G, I164V
Sel III		A3076G, E213E T3301G, G288G	A3965T, M63L	A4782G, D236G	G6297A, S121N G6523A, E196E T6934C, A333A

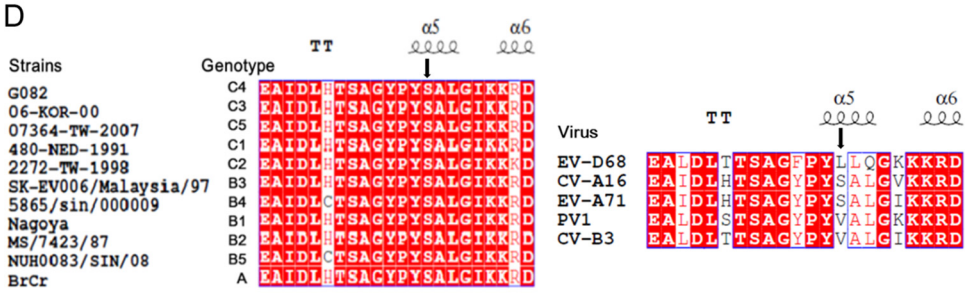

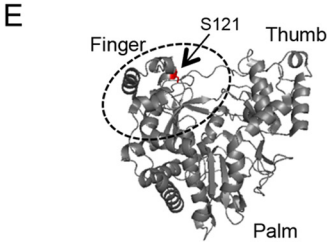

above. For each drug combination, the two compounds were prepared separately by serial 2-fold dilution and were mixed in 96-well plates (without using the edges of the plates) to create a 6-by-9 matrix of single and combined diluted drugs. The drug serial dilutions spanned a range of concentrations near each compound's EC_{50} so that equivalent antiviral activities were compared. Cell control wells containing medium only and virus control wells without compound treatment were included in each plate, and each combination was tested four times in at least three independent experiments. The cytotoxicity of each combination was assessed in parallel by determination of the viability of uninfected cells using CellTiter-Glo reagent (Promega).

Analysis of drug combination effects. To assess the antiviral effects of different drug combinations, volumes of synergy or antagonism were determined by using the MacSynergy II program developed by Prichard and Shipman (43). This program is based on the Bliss independent model. The synergy/antagonism volumes ($\mu M^2\%$) of drug combinations at 95% confidence were defined as follows: values between −25 and +25 indicate additivity, and values between +25 and +50 or between −25 and −50 indicate minor but significant synergy or antagonism, respectively, whereas values between +50 and +100 or between −50 and −100 are interpreted as moderate synergism or antagonism, respectively. Values greater than +100 or less than −100 indicate strong synergistic or antag-

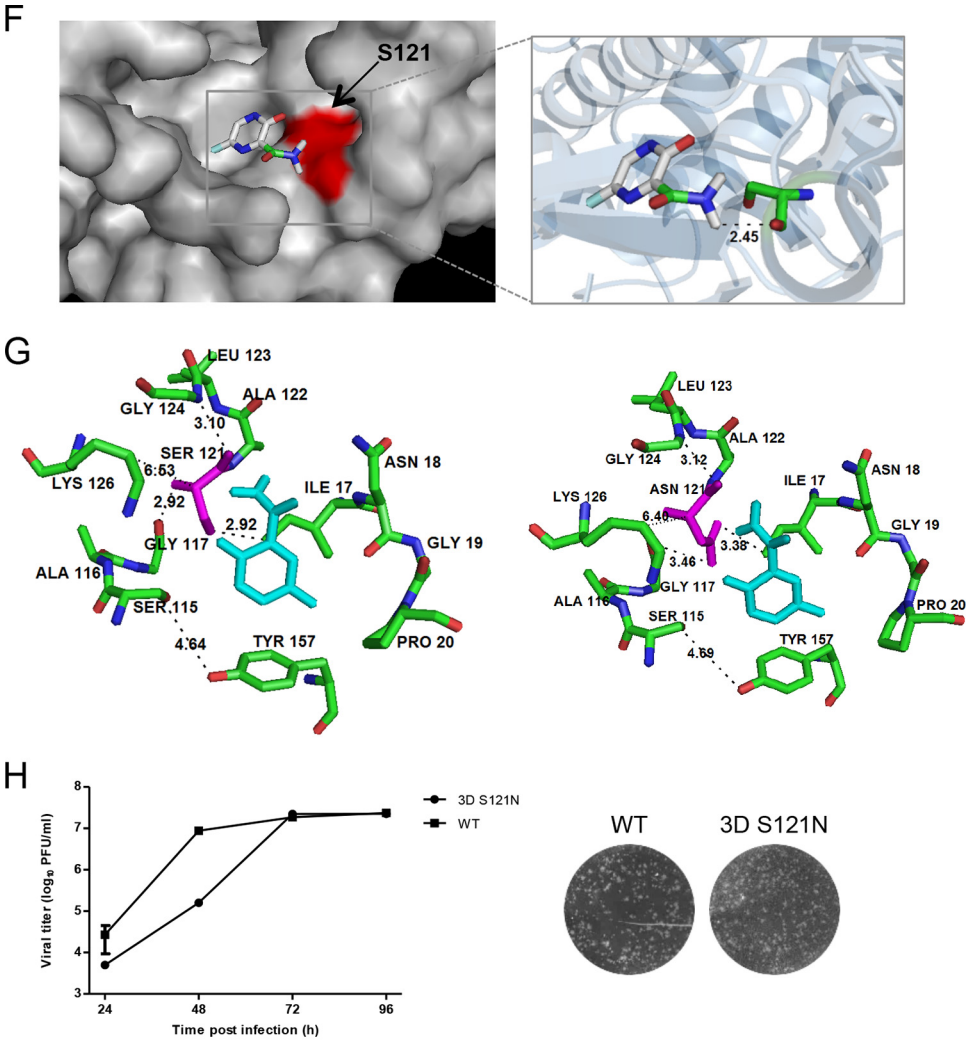

FIG 2 Mutation in EV-A71 3D polymerase confers resistance to favipiravir. (A) Scheme for the selection of favipiravir-resistant virus. (B) Resistance analysis by a virus yield reduction assay. Vero cells were infected with the WT virus, P16 selections (Sel I and Sel III), or the 3D S121N mutant virus in the presence of 600 μM favipiravir or 0.25% DMSO (as a negative control). At 48 h postinfection, the viral titers in culture fluids were quantified by a plaque assay. Fold reduction was determined by dividing the titer of virus treated with 0.25% DMSO by that of virus treated with 600 μM favipiravir. Resistance is quantified by the fold change compared to the wild-type virus, which was set as 1.0. (C) Summary of mutations identified from the two selections. Locations of the nucleotide and/or amino acid changes are indicated. (D) Sequence alignment of the resistance regions in 3D proteins of representative strains of EV-A71 genotypes (left) (the name of each EV-A71 strain of genotypes A, B1, B2, B3, B4, B5, C1, C2, C3, C4, and C5 is indicated on the left) and members of the genus *Enterovirus* (right) (sequences with GenBank accession no. EU262658 [CV-A16], M33854 [CV-B3], KF537633 [PV1], and KF726085 [EV-D68] were used). The arrow indicates the mutation in favipiravir-resistant EV-A71 identified in this study. The secondary structure based on the structure model of the EV-A71 3D polymerase (Protein Data Bank accession no. 3N6L) is shown above the sequence. (E) Location of the S121 mutation in the structural model of EV-A71 3D polymerase. Residue S121 is shown in red. The figure was produced by using PyMOL. (F) Modeling of favipiravir into the finger subdomain of EV-A71 3D polymerase. (Left) Favipiravir (represented in stick form and colored in atoms) was docked into the structure of EV-A71 $3D^{pol}$ (Protein Data Bank accession no. 3N6L) (gray) by using Autodock Vina, and the lowest-energy conformation is presented. Residue S121 is shown in red. (Right) Partial structure of the $3D^{pol}$ finger subdomain represented as a cartoon. Residue S121 is highlighted in a stick representation, with carbon atoms in green. The image was generated by using PyMOL. (G) Modeling of the favipiravir-resistant mutation. (Left) The polymerase residues in contact with favipiravir are shown with carbon atoms in green and explicitly labeled. (Right) Structural model of the 3D S121N mutation generated by using SWISS-MODEL. Favipiravir is shown in cyan, and both residues S121 and N121 are shown in magenta. Images were created by using PyMOL. (H) Phenotypic characterization of the resistance mutant. (Left) Growth kinetics of wild-type EV-A71 and the 3D S121N mutant virus. The data shown were obtained from two independent replicates. Error bars indicate the standard deviations from two independent experiments. (Right) Plaque phenotypes of wild-type EV-A71 and the 3D S121N mutant virus.

onistic activity, respectively. To assess the effect of the combination of rupintrivir and ITZ on EV-A71 yield, drug combinations were analyzed at two constant ratios. Combination indices (CIs) were calculated with the Chou-Talalay method using Compusyn software, and CI values of <1, 1, and >1 indicate synergy, additivity, and antagonism between drugs, respectively (44).

RESULTS

Antiviral activity of individual compounds. Five compounds (suramin, ITZ, GW5074, rupintrivir, and favipiravir) with distinct mechanisms of action and different resistance profiles (see the introduction) were chosen to test their combined antiviral

TABLE 1 Cross-resistance profiling of inhibitors of ITZ- and favipiravir-resistant viruses

Compound	Mean EC_{50} (μM) for WT ± SD	3A V51L + V75A		3D S121N	
		Mean EC_{50} (μM) ± SD	Shift (*n*-fold)[a]	Mean EC_{50} (μM) ± SD	Shift (*n*-fold)[a]
Suramin	9.55 ± 0.18	13.05 ± 0.96	1.37	6.19 ± 0.17	0.65
ITZ	0.36 ± 0.02	1.31 ± 0.02	3.64	0.49 ± 0.003	1.36
GW5074	1.7 ± 0.0007	2.91 ± 0.47	1.71	0.77 ± 0.07	0.45
Rupintrivir	0.18 ± 0.006	0.22 ± 0.04	1.22	0.05 ± 0.05	0.28
Favipiravir	145.6 ± 7.57	171 ± 5.66	1.17	318.1 ± 39.87	2.18

[a] Susceptibility data are expressed as the shift in the EC_{50} of mutants compared to the wild type. Shifts in the EC_{50} of >2-fold were considered to indicate cross-resistance.

activities against EV-A71. We first determined the anti-EV-A71 activities of individual compounds as well as their cytotoxicities in order to obtain an optimal range of compound concentrations for use in combination studies. A CPE-based antiviral activity assay was used to measure antiviral activity. As shown in Fig. 1A, each of the selected compounds inhibited the EV-A71-induced CPE in a dose-responsive manner without significant cytotoxicity. Among these compounds, rupintrivir was the most potent, with an EC_{50} of 0.18 μM. Next, we used a virus yield reduction assay to validate the inhibitory effect. Suramin, ITZ, GW5074, rupintrivir, and favipiravir reduced viral titers by 3.7, 1.6, 1.5, 4.2, and 1.8 $\log_{10}$ units at highest test concentrations, respectively (Fig. 1B). The results demonstrated that all selected compounds have anti-EV-A71 activity with an SI of >10 in cell culture.

The 3D polymerase of EV-A71 is the molecular target of favipiravir. Favipiravir was recently reported to be a weak inhibitor of the *in vitro* replication of EV-D68 (31). We found that it could also inhibit EV-A71 replication with an EC_{50} of 68.74 μM in a CPE assay (Fig. 1A). To gain insight into the mechanism by which favipiravir inhibits the replication of enterovirus, we generated favipiravir-resistant virus variants by culturing EV-A71 with increasing concentrations of favipiravir (Fig. 2A). We performed three independent selections in parallel, and only two selections (selection I [Sel I] and Sel III) showed a resistance phenotype after 16 passages. Compared to the WT, the Sel I and Sel III viruses were partially resistant to favipiravir (Fig. 2B, left). At 600 μM favipiravir, the Sel I and Sel III viruses generated fold changes of 47.8- and 6.9-fold compared to the WT, respectively (Fig. 2B, right). Whole-genome sequence analysis revealed that up to 7 mutations were observed in both Sel I and Sel III (Fig. 2C), and the 3D S121N mutation was the only common mutation, indicating that the 3D protein could be the potential target of favipiravir. In addition to mutations in the 3D protein, additional mutations were also detected in the VP2, VP1, 2B, and 2C regions. As a negative control, viruses passaged in 0.25% DMSO had a VP1 T237N mutation but did not exhibit the mutations found in Sel I and Sel III. The 3D protein acts as a viral RNA-dependent RNA polymerase (RdRp) and plays a major role in viral genome replication (45–47). To evaluate whether the 3D S121N mutation could confer resistance to favipiravir, we introduced the mutation into an infectious cDNA clone. Compared to the WT, the 3D S121N mutant virus generated changes of 9.9-fold in the presence of 600 μM favipiravir (Fig. 2B), demonstrating that the 3D S121N single mutation conferred EV-A71 resistance to favipiravir.

Sequence alignment of the 3D polymerase showed that residue S121 is completely conserved among 11 genotypes of EV-A71 (A, B1 to B5, and C1 to C5) and CV-A16, whereas CV-B3 and PV1 encoded V and EV-D68 encoded L at this position (Fig. 2D). On the structure model of the EV-A71 3D polymerase, residue S121 is located in the finger subdomain (Fig. 2E). Computer modeling of favipiravir into the finger subdomain of the EV-A71 3D polymerase revealed that the amine group of favipiravir interacts with residue S121 (Fig. 2F). Favipiravir contact residues in the 3D polymerase are shown in Fig. 2G. The replacement of serine by asparagine at position 121 could result in a greater distance between the residue and compound, which in turn may weaken the interaction of the residue with the compound.

Multistep growth curves for the 3D S121N mutant virus showed that it replicated more slowly than the WT at early time points (24 and 48 h postinfection) but could achieve similar peak titers from 72 h postinfection, and it displayed plaque morphology similar to that of the WT, suggesting that the mutation slightly affect replication kinetics (Fig. 2H). Furthermore, the 3D S121N mutation was retained after three passages in Vero cells (data not shown), indicating that the mutant virus was genetically stable.

Viruses resistant to ITZ or favipiravir remain susceptible to other inhibitors. We previously found that ITZ-resistant viruses contained mutations in nonstructural protein 3A, and 3A V51L and 3A V75A mutant viruses exhibited 2.56- and 3.42-fold shifts in EC_{50}s in a CPE assay, respectively (24). Here, we reverse engineered a mutant virus containing a double mutation (3A V51L V75A) and found that the virus exhibited slightly greater resistance to ITZ, with a 3.64-fold shift in the EC_{50} in the CPE assay (Table 1). We therefore used this double mutant for cross-resistance phenotyping. We performed a CPE assay on Vero cells, as described previously (24), to evaluate whether the ITZ- and favipiravir-resistant viruses remained susceptible to other selected inhibitors. As summarized in Table 1, there were no significant shifts (<2-fold) in EC_{50}s against other inhibitors for both the 3A V51L V75A and 3D S121N mutant viruses, suggesting that viruses resistant to ITZ or favipiravir are still susceptible to other inhibitors.

Antiviral activities and cytotoxic effects of two-drug combinations. We measured anti-EV-A71 activities of different compound pairs in a checkerboard format using a CPE assay. To assess whether the observed antiviral activities of the drug combinations were synergistic, antagonistic, or simply additive, the experimental data were analyzed with the MacSynergy II program. This program calculated the theoretical additive interactions of the drugs based on the Bliss independence theory and displayed synergy and antagonism as peaks above or below a predicted additive plane in a three-dimensional graph (43). The graphs in Fig. 3 show the results for each of the drug combinations analyzed. The corresponding mean volumes of synergy and antagonism at the 95%

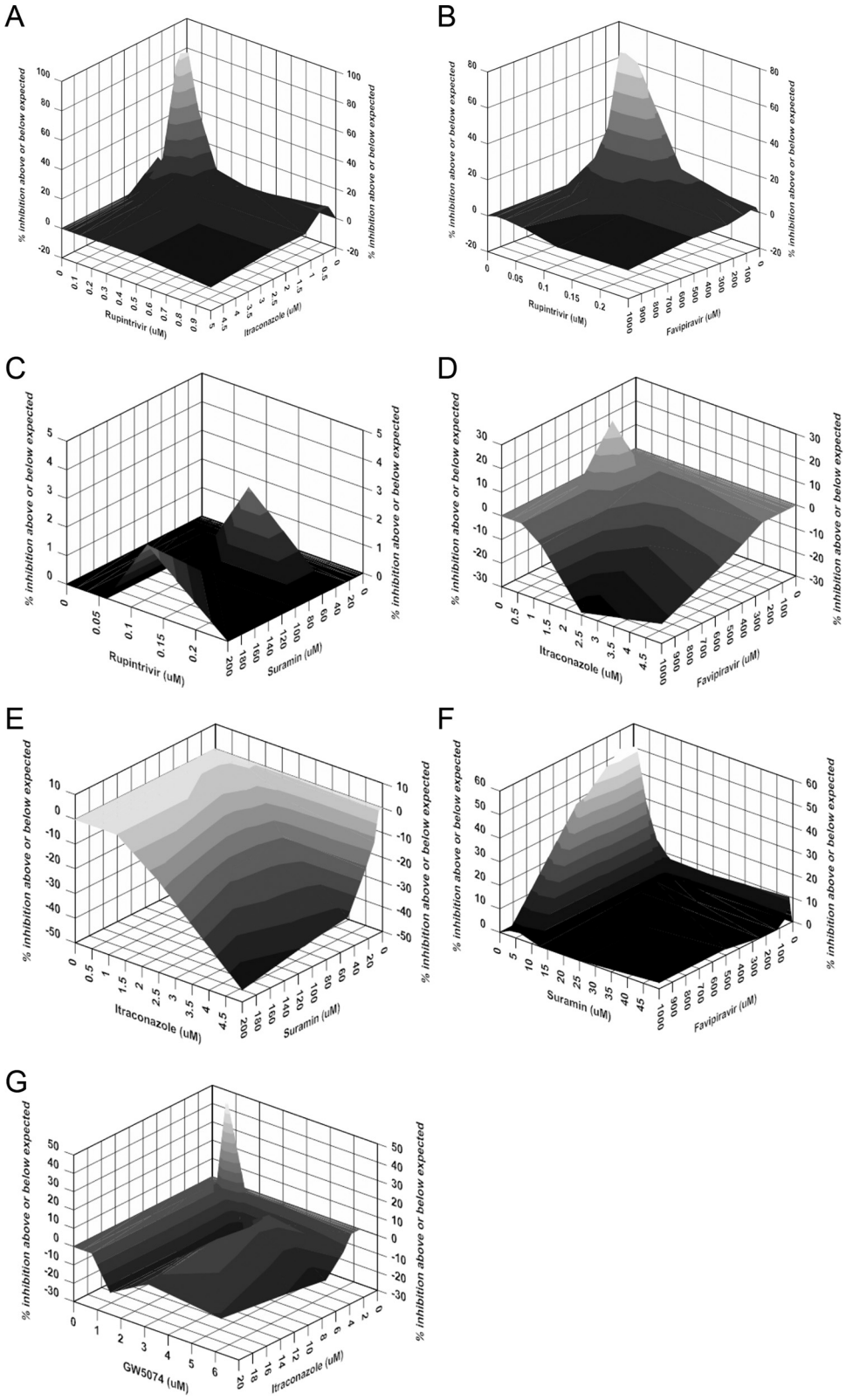

FIG 3 Analysis of drug combinations using the MacSynergy II program. Data shown were obtained at the 95% confidence level and were plotted with DeltaGraph. Values in the zero plane indicate additive activity, values under the zero plane indicate antagonistic activity, and values above the zero plane indicate synergistic activity. Combinations of rupintrivir plus itraconazole (A), favipiravir (B), and suramin (C); combinations of itraconazole plus favipiravir (D) and suramin (E); the combination of suramin plus favipiravir (F); and the combination of GW5074 plus itraconazole (G) are presented. All data points are averages of four measurements from at least three independent experiments.

TABLE 2 Interactions of drug-drug combinations against EV-A71

Drug combination	Synergy/antagonism ($\mu M^2\%$)[a] by MacSynergy II analysis	Predicted interaction
Rupintrivir + ITZ	450.64/−4.04	Strong synergy
Rupintrivir + favipiravir	438.07/−8.36	Strong synergy
Rupintrivir + suramin	4.96/0	Additivity
ITZ + favipiravir	34.51/−88.11	Moderate antagonism, minor synergy
ITZ + suramin	0.14/−246.23	Strong antagonism
Suramin + favipiravir	337.59/0	Strong synergy
GW5074 + ITZ	53.91/−167.68	Strong antagonism, moderate synergy

[a] Mean volumes of synergy or antagonism are presented based on 95% confidence levels.

confidence level are summarized in Table 2. When ITZ and favipiravir were individually combined with rupintrivir, the volumes of synergy were extremely high (450.64 and 438.07 $\mu M^2\%$, respectively), indicating a strong synergistic effect, while when suramin was combined with rupintrivir, an additive effect was observed. In contrast to the combination of suramin and favipiravir, which yielded a strong synergistic effect, the combination of suramin and ITZ resulted in a strong antagonistic effect. The combination of ITZ and favipiravir was complex, showing minor synergy but with a moderate level of antagonism. The combination of ITZ and GW5074 showed moderate synergy at low concentrations and strong antagonism at high concentrations. Of note, all combination studies included concurrent evaluations of cell viability, and none of the synergistic and additive combinations showed synergistic cytotoxicity within the range of drug concentrations examined, while the remaining combinations showed increased but not significant cytotoxicity (>60% cell viability at all tested doses [data not shown]). The extent of the synergy volume of three combinations (rupintrivir plus ITZ, rupintrivir plus favipiravir, and suramin plus favipiravir) indicates that these effects are probably important *in vivo*.

Combination of rupintrivir and ITZ synergistically reduces EV-A71 yield. Because the combination of rupintrivir and ITZ exhibited the strongest synergistic effect on EV-A71-induced CPE inhibition, we further evaluated this combination in a virus yield reduction assay. Vero cells were infected with EV-A71 strain G082 and treated with ITZ and rupintrivir at constant ratios (1:0.1 and 1:0.05), and viral titers were determined by a plaque assay. The antiviral effects produced by the combination of rupintrivir and ITZ at two fixed ratios of concentrations were compared to those produced by rupintrivir or ITZ alone. The dose-effect relationships were assessed by a method developed by Chou using Compusyn software (44). CIs were calculated at the EC_{50}, EC_{75}, EC_{90}, and EC_{95} levels. As summarized in Table 3, very strong synergism was obtained at a 1:0.1 ratio, with CIs ranging from 0.01 to 0.03, and strong synergism was obtained at a 1:0.05 ratio, with a CI of 0.21. This result was consistent with the clear synergistic drug interaction observed in the MacSynergy evaluation. In summary, the antiviral interaction between rupintrivir and ITZ was synergistic.

Rupintrivir suppresses emergence of resistance against ITZ. In general, the use of antiviral agents with different resistance profiles in combination creates a higher genetic barrier to the development of resistance, thereby suppressing the emergence of resistance. We studied whether rupintrivir is able to delay or even prevent resistance development of EV-A71 against ITZ. By using the same scheme for the selection of ITZ-resistant viruses (24), EV-A71 was cultured in the presence of ITZ alone or in combination with rupintrivir. ITZ-resistant EV-A71 variants were readily selected at P16, as we found previously (24); however, when ITZ was combined with 0.5 μM or 1 μM rupintrivir, no apparent CPE was observed at P16 for all three independent selections. The P16 viruses were then cultured for four more consecutive passages under the same conditions as those for P16; however, no apparent CPE was observed (data not shown). We then detected the viruses at P10, P16, and P20 using RT-PCR targeting the VP1 gene, a plaque assay, and an infectious-center assay as described previously (42). Surprisingly, the virus became undetectable, suggesting that EV-A71 was completely inhibited by treatment with the combination of rupintrivir and ITZ. It should be noted that the combination of rupintrivir and ITZ did not cause an adverse effect on Vero cells since no changes in morphology or density were observed in parallel control cultures. Thus, the combination of rupintrivir and ITZ completely cleared EV-A71 infection from cell culture and prevented the emergence of resistance.

TABLE 3 Dose-effect relationships of the combination of ITZ and rupintrivir

ITZ/rupintrivir ratio[a]	% inhibition (ED_n)[b]	CI[c] (interaction)	DRI[d]	
			ITZ	Rupintrivir
1:0.1	50	0.01 (very strong synergism)	285.69	138.38
	75	0.01 (very strong synergism)	212.18	89.31
	90	0.02 (very strong synergism)	157.58	57.64
	95	0.03 (very strong synergism)	128.72	42.79
1:0.05	50	0.21 (strong synergism)	9.51	9.22
	75	0.21 (strong synergism)	10.34	8.71
	90	0.21 (strong synergism)	11.24	8.22
	95	0.21 (strong synergism)	11.90	7.91

[a] Drugs were tested at constant ratios (1:0.1 and 1:0.05).
[b] ED_n indicates the effective dose at the EC_{50}, EC_{75}, EC_{90}, and EC_{95} levels.
[c] The combination index (CI) was calculated by using Compusyn software. CIs of <1, 1, and >1 indicate synergism, an additive effect, and antagonism, respectively, at different effective doses. A CI of <0.1 indicates very strong synergism, and values between 0.1 and 0.3 indicate strong synergism.
[d] The dose reduction index (DRI) is the fold dose reduction allowed for a drug combination to reach a given degree of inhibition compared to the drug as a single agent.

DISCUSSION

There is still a great need for an effective treatment to address the medical and economic burden of EV-A71 infection. The facts that several enterovirus inhibitors failed in clinical trials, mainly due to safety issues (e.g., enviroxime) and an insufficient therapeutic effect (e.g., rupintrivir), and that the industry has put less effort into developing enterovirus inhibitors since the 1990s have hampered the progress of antienterovirus drug development. Therefore, a new strategy to repurpose old drugs and use multiple antiviral agents with additive or synergistic antiviral effects in combination may be a good solution by improving antiviral potency, minimizing potential side effects, and saving time and cost. Both drug repurposing and combination therapy were valid approaches. Recently, combination therapy targeting different steps of the enterovirus replication cycle has shown synergistic activity (48). One of the main goals of our study was to evaluate the combination effects of compounds with antienterovirus activity that are FDA approved or have reached clinical trials.

In this study, we selected five compounds based on their different mechanisms of action for combination studies. Among them, suramin and ITZ were approved by the FDA for the treatment of human sleeping sickness caused by trypanosomes and fungal infections, respectively; favipiravir was approved in Japan for the treatment of infections with influenza virus; and rupintrivir completed a phase II clinical trial. We performed two-drug combination experiments for these four compounds. Interestingly, the combination of rupintrivir and any of the three other compounds yielded at least additive antiviral effects in six pairs of combinations. This might be because rupintrivir targets the 3C protease and does not interfere with the mechanisms of the other compounds. A previous study also showed that the combination of rupintrivir and interferon exerted strong synergistic anti-EV-A71 activity (49). In addition, we evaluated the combination of ITZ and GW5074. Although they belong to different classes of enviroxime-like compounds and target different host factors (25, 50), their resistance mutations were located in the 3A protein (23, 24), a small hydrophobic protein (86 to 89 amino acids). It is likely that the molecules compete with each other in the interaction of the 3A protein with host factors at high concentrations, resulting in the observed strong antagonism effect.

The second part of this study consisted of identifying potential inhibitory mechanism of favipiravir against enterovirus. We generated favipiravir-resistant EV-A71 variants and confirmed that the 3D S121N mutation could confer partial resistance to favipiravir using a reverse genetic approach. Interestingly, the serine at position 121 in $3D^{Pol}$ is completely conserved among all genotypes of EV-A71. Compared to Sel III, Sel I carried two more mutations that resulted in an amino acid change in $3D^{Pol}$ (S96G and I164V) (Fig. 2C), which may be associated with the higher level of resistance of Sel I (Fig. 2B), although the contribution of these two mutations needs to be further validated. These findings together with the previous identification of a favipiravir resistance mutation in the RdRp nsP4 of chikungunya virus (34) suggest that $3D^{Pol}$ of EV-A71 is the target of favipiravir. A modeling study was performed to elucidate the role of the amino acid substitution S121N in $3D^{Pol}$ in antiviral resistance (Fig. 2F and G). In $3D^{Pol}$, the residue at position 121 maps to the "pinky" finger domain, which is separated from the other fingers by a groove at the top of the finger domain (51). A possible explanation for the effect of the serine-to-asparagine substitution that results in resistance is that the greater distance between residue N121 and favipiravir could weaken the interaction of the residue with the compound, resulting in resistance. However, the precise resistance mechanism needs to be further determined by elucidation of the crystal structure of favipiravir bound to EV-A71 $3D^{Pol}$ and *in vitro* polymerase activity assays.

A greater genetic barrier to the emergence of viral escape mutants is a key advantage of antiviral therapies. Although resistance to enterovirus inhibitors has not been reported in clinical studies, compound-resistant viruses were readily isolated in the laboratory. We found that rupintrivir is highly effective in suppressing the emergence of resistance when used in combination with ITZ, suggesting that this combination may reduce the risk of generating drug-resistant mutants in the clinical management of EV-A71 infections.

In summary, three of the analyzed two-drug combinations (i.e., rupintrivir plus ITZ, rupintrivir plus favipiravir, and suramin plus favipiravir) yielded strong synergistic antiviral effects, and none of these combinations exhibited synergistic cytotoxicity in cell culture. Further *in vivo* investigation is warranted. Since rupintrivir and ITZ are broad-spectrum enterovirus replication inhibitors, it will be of interest to see whether a similar effect can be achieved for other members of the *Enterovirus* genus. Moreover, we provided evidence for favipiravir targeting the RdRp of RNA viruses by the identification of a specific resistance mutation in $3D^{Pol}$ of EV-A71, and the inhibitory and resistance mechanisms should be investigated further by elucidation of the structure of $3D^{Pol}$ of EV-A71 in complex with an inhibitor.

ACKNOWLEDGMENTS

We thank all the laboratory members for technical support and helpful discussions during the study.

This research was partially supported by funding from the Total Foundation, the National Natural Science Foundation of China (grant no. 31400148), the Science and Technology Commission of Shanghai Municipality (grant no. 14YF1407600), and the CAS-SIBS Frontier Research Field Foundation for Young Scientists (grant no. 2014KIP109). G.Z. gratefully acknowledges the support of the SA-SIBS scholarship program.

FUNDING INFORMATION

This work, including the efforts of Gang Zou, was funded by National Natural Science Foundation of China (NSFC) (31400148). This work, including the efforts of Gang Zou, was funded by Science and Technology Commission of Shanghai Municipality (STCSM) (14YF1407600).

The funders had no role in study design, data collection and interpretation, or the decision to submit the work for publication.

REFERENCES

1. **Chang LY, Lin TY, Hsu KH, Huang YC, Lin KL, Hsueh C, Shih SR, Ning HC, Hwang MS, Wang HS, Lee CY.** 1999. Clinical features and risk factors of pulmonary oedema after enterovirus-71-related hand, foot, and mouth disease. Lancet **354:**1682–1686. http://dx.doi.org/10.1016/S0140-6736(99)04434-7.
2. **Ooi MH, Wong SC, Lewthwaite P, Cardosa MJ, Solomon T.** 2010. Clinical features, diagnosis, and management of enterovirus 71. Lancet Neurol **9:**1097–1105. http://dx.doi.org/10.1016/S1474-4422(10)70209-X.
3. **Xing W, Liao Q, Viboud C, Zhang J, Sun J, Wu JT, Chang Z, Liu F, Fang VJ, Zheng Y, Cowling BJ, Varma JK, Farrar JJ, Leung GM, Yu H.** 2014. Hand, foot, and mouth disease in China, 2008-12: an epidemiological study. Lancet Infect Dis **14:**308–318. http://dx.doi.org/10.1016/S1473-3099(13)70342-6.
4. **McMinn P, Stratov I, Nagarajan L, Davis S.** 2001. Neurological mani-

festations of enterovirus 71 infection in children during an outbreak of hand, foot, and mouth disease in Western Australia. Clin Infect Dis **32:** 236–242. http://dx.doi.org/10.1086/318454.
5. **Zhang Q, Macdonald NE, Smith JC, Cai K, Yu H, Li H, Lei C.** 2014. Severe enterovirus type 71 nervous system infections in children in the Shanghai region of China: clinical manifestations and implications for prevention and care. Pediatr Infect Dis J **33:**482–487. http://dx.doi.org/10.1097/INF.0000000000000194.
6. **Shimizu H, Nakashima K.** 2014. Surveillance of hand, foot, and mouth disease for a vaccine. Lancet Infect Dis **14:**262–263. http://dx.doi.org/10.1016/S1473-3099(13)70330-X.
7. **Ho M, Chen ER, Hsu KH, Twu SJ, Chen KT, Tsai SF, Wang JR, Shih SR.** 1999. An epidemic of enterovirus 71 infection in Taiwan. Taiwan Enterovirus Epidemic Working Group. N Engl J Med **341:**929–935.
8. **Chan KP, Goh KT, Chong CY, Teo ES, Lau G, Ling AE.** 2003. Epidemic hand, foot and mouth disease caused by human enterovirus 71, Singapore. Emerg Infect Dis **9:**78–85. http://dx.doi.org/10.3201/eid1301.020112.
9. **Tu PV, Thao NT, Perera D, Huu TK, Tien NT, Thuong TC, How OM, Cardosa MJ, McMinn PC.** 2007. Epidemiologic and virologic investigation of hand, foot, and mouth disease, southern Vietnam, 2005. Emerg Infect Dis **13:**1733–1741. http://dx.doi.org/10.3201/eid1311.070632.
10. **Zhang Y, Zhu Z, Yang W, Ren J, Tan X, Wang Y, Mao N, Xu S, Zhu S, Cui A, Yan D, Li Q, Dong X, Zhang J, Zhao Y, Wan J, Feng Z, Sun J, Wang S, Li D, Xu W.** 2010. An emerging recombinant human enterovirus 71 responsible for the 2008 outbreak of hand foot and mouth disease in Fuyang city of China. Virol J **7:**94. http://dx.doi.org/10.1186/1743-422X-7-94.
11. **Seiff A.** 2012. Cambodia unravels cause of mystery illness. Lancet **380:**206.
12. **Ma E, Chan KC, Cheng P, Wong C, Chuang SK.** 2010. The enterovirus 71 epidemic in 2008—public health implications for Hong Kong. Int J Infect Dis **14:**e775–e780. http://dx.doi.org/10.1016/j.ijid.2010.02.2265.
13. **Wimmer E, Hellen CU, Cao X.** 1993. Genetics of poliovirus. Annu Rev Genet **27:**353–436. http://dx.doi.org/10.1146/annurev.ge.27.120193.002033.
14. **De Palma AM, Vliegen I, De Clercq E, Neyts J.** 2008. Selective inhibitors of picornavirus replication. Med Res Rev **28:**823–884. http://dx.doi.org/10.1002/med.20125.
15. **Abzug MJ.** 2014. The enteroviruses: problems in need of treatments. J Infect **68**(Suppl 1)**:**S108–S114. http://dx.doi.org/10.1016/j.jinf.2013.09.020.
16. **van der Linden L, Wolthers KC, van Kuppeveld FJ.** 2015. Replication and inhibitors of enteroviruses and parechoviruses. Viruses **7:**4529–4562. http://dx.doi.org/10.3390/v7082832.
17. **Tan CW, Lai JK, Sam IC, Chan YF.** 2014. Recent developments in antiviral agents against enterovirus 71 infection. J Biomed Sci **21:**14. http://dx.doi.org/10.1186/1423-0127-21-14.
18. **Wang Y, Qing J, Sun Y, Rao Z.** 2014. Suramin inhibits EV71 infection. Antiviral Res **103:**1–6. http://dx.doi.org/10.1016/j.antiviral.2013.12.008.
19. **Ren P, Zou G, Bailly B, Xu S, Zeng M, Chen X, Sheng L, Zhang Y, Guillon P, Arenzana-Seisdedos F, Buchy P, Li J, von Itzstein M, Li Q, Altmeyer R.** 2014. The approved pediatric drug suramin identified as a clinical candidate for the treatment of EV71 infection—suramin inhibits EV71 infection in vitro & in vivo. Emerg Microbes Infect **3:**e62. http://dx.doi.org/10.1038/emi.2014.60.
20. **Tan CW, Poh CL, Sam IC, Chan YF.** 2013. Enterovirus 71 uses cell surface heparan sulfate glycosaminoglycan as an attachment receptor. J Virol **87:**611–620. http://dx.doi.org/10.1128/JVI.02226-12.
21. **Arita M, Wakita T, Shimizu H.** 2008. Characterization of pharmacologically active compounds that inhibit poliovirus and enterovirus 71 infectivity. J Gen Virol **89:**2518–2530. http://dx.doi.org/10.1099/vir.0.2008/002915-0.
22. **Nishimura Y, McLaughlin NP, Pan J, Goldstein S, Hafenstein S, Shimizu H, Winkler JD, Bergelson JM.** 2015. The suramin derivative NF449 interacts with the 5-fold vertex of the enterovirus A71 capsid to prevent virus attachment to PSGL-1 and heparan sulfate. PLoS Pathog **11:** e1005184. http://dx.doi.org/10.1371/journal.ppat.1005184.
23. **Strating JR, van der Linden L, Albulescu L, Bigay J, Arita M, Delang L, Leyssen P, van der Schaar HM, Lanke KH, Thibaut HJ, Ulferts R, Drin G, Schlinck N, Wubbolts RW, Sever N, Head SA, Liu JO, Beachy PA, De Matteis MA, Shair MD, Olkkonen VM, Neyts J, van Kuppeveld FJ.** 2015. Itraconazole inhibits enterovirus replication by targeting the oxysterol-binding protein. Cell Rep **10:**600–615. http://dx.doi.org/10.1016/j.celrep.2014.12.054.
24. **Gao Q, Yuan S, Zhang C, Wang Y, Wang Y, He G, Zhang S, Altmeyer R, Zou G.** 2015. Discovery of itraconazole with broad-spectrum in vitro antienterovirus activity that targets nonstructural protein 3A. Antimicrob Agents Chemother **59:**2654–2665. http://dx.doi.org/10.1128/AAC.05108-14.
25. **Arita M, Kojima H, Nagano T, Okabe T, Wakita T, Shimizu H.** 2011. Phosphatidylinositol 4-kinase III beta is a target of enviroxime-like compounds for antipoliovirus activity. J Virol **85:**2364–2372. http://dx.doi.org/10.1128/JVI.02249-10.
26. **van der Schaar HM, van der Linden L, Lanke KH, Strating JR, Purstinger G, de Vries E, de Haan CA, Neyts J, van Kuppeveld FJ.** 2012. Coxsackievirus mutants that can bypass host factor PI4KIIIbeta and the need for high levels of PI4P lipids for replication. Cell Res **22:**1576–1592. http://dx.doi.org/10.1038/cr.2012.129.
27. **Arita M, Wakita T, Shimizu H.** 2009. Cellular kinase inhibitors that suppress enterovirus replication have a conserved target in viral protein 3A similar to that of enviroxime. J Gen Virol **90:**1869–1879. http://dx.doi.org/10.1099/vir.0.012096-0.
28. **Binford SL, Maldonado F, Brothers MA, Weady PT, Zalman LS, Meador JW, III, Matthews DA, Patick AK.** 2005. Conservation of amino acids in human rhinovirus 3C protease correlates with broad-spectrum antiviral activity of rupintrivir, a novel human rhinovirus 3C protease inhibitor. Antimicrob Agents Chemother **49:**619–626. http://dx.doi.org/10.1128/AAC.49.2.619-626.2005.
29. **Matthews DA, Dragovich PS, Webber SE, Fuhrman SA, Patick AK, Zalman LS, Hendrickson TF, Love RA, Prins TJ, Marakovits JT, Zhou R, Tikhe J, Ford CE, Meador JW, Ferre RA, Brown EL, Binford SL, Brothers MA, DeLisle DM, Worland ST.** 1999. Structure-assisted design of mechanism-based irreversible inhibitors of human rhinovirus 3C protease with potent antiviral activity against multiple rhinovirus serotypes. Proc Natl Acad Sci U S A **96:**11000–11007. http://dx.doi.org/10.1073/pnas.96.20.11000.
30. **Patick AK, Binford SL, Brothers MA, Jackson RL, Ford CE, Diem MD, Maldonado F, Dragovich PS, Zhou R, Prins TJ, Fuhrman SA, Meador JW, Zalman LS, Matthews DA, Worland ST.** 1999. In vitro antiviral activity of AG7088, a potent inhibitor of human rhinovirus 3C protease. Antimicrob Agents Chemother **43:**2444–2450.
31. **Sun L, Meijer A, Froeyen M, Zhang L, Thibaut HJ, Baggen J, George S, Vernachio J, van Kuppeveld FJ, Leyssen P, Hilgenfeld R, Neyts J, Delang L.** 2015. Antiviral activity of broad-spectrum and enterovirus-specific inhibitors against clinical isolates of enterovirus D68. Antimicrob Agents Chemother **59:**7782–7785. http://dx.doi.org/10.1128/AAC.01375-15.
32. **Furuta Y, Takahashi K, Fukuda Y, Kuno M, Kamiyama T, Kozaki K, Nomura N, Egawa H, Minami S, Watanabe Y, Narita H, Shiraki K.** 2002. In vitro and in vivo activities of anti-influenza virus compound T-705. Antimicrob Agents Chemother **46:**977–981. http://dx.doi.org/10.1128/AAC.46.4.977-981.2002.
33. **Julander JG, Smee DF, Morrey JD, Furuta Y.** 2009. Effect of T-705 treatment on Western equine encephalitis in a mouse model. Antiviral Res **82:**169–171. http://dx.doi.org/10.1016/j.antiviral.2009.02.201.
34. **Delang L, Segura Guerrero N, Tas A, Querat G, Pastorino B, Froeyen M, Dallmeier K, Jochmans D, Herdewijn P, Bello F, Snijder EJ, de Lamballerie X, Martina B, Neyts J, van Hemert MJ, Leyssen P.** 2014. Mutations in the chikungunya virus non-structural proteins cause resistance to favipiravir (T-705), a broad-spectrum antiviral. J Antimicrob Chemother **69:**2770–2784. http://dx.doi.org/10.1093/jac/dku209.
35. **Gowen BB, Wong MH, Jung KH, Sanders AB, Mendenhall M, Bailey KW, Furuta Y, Sidwell RW.** 2007. In vitro and in vivo activities of T-705 against arenavirus and bunyavirus infections. Antimicrob Agents Chemother **51:**3168–3176. http://dx.doi.org/10.1128/AAC.00356-07.
36. **Mendenhall M, Russell A, Smee DF, Hall JO, Skirpstunas R, Furuta Y, Gowen BB.** 2011. Effective oral favipiravir (T-705) therapy initiated after the onset of clinical disease in a model of arenavirus hemorrhagic fever. PLoS Negl Trop Dis **5:**e1342. http://dx.doi.org/10.1371/journal.pntd.0001342.
37. **Rocha-Pereira J, Jochmans D, Dallmeier K, Leyssen P, Nascimento MS, Neyts J.** 2012. Favipiravir (T-705) inhibits in vitro norovirus replication. Biochem Biophys Res Commun **424:**777–780. http://dx.doi.org/10.1016/j.bbrc.2012.07.034.
38. **Smither SJ, Eastaugh LS, Steward JA, Nelson M, Lenk RP, Lever MS.** 2014. Post-exposure efficacy of oral T-705 (favipiravir) against inhalational Ebola virus infection in a mouse model. Antiviral Res **104:**153–155. http://dx.doi.org/10.1016/j.antiviral.2014.01.012.
39. **Julander JG, Shafer K, Smee DF, Morrey JD, Furuta Y.** 2009. Activity of

T-705 in a hamster model of yellow fever virus infection in comparison with that of a chemically related compound, T-1106. Antimicrob Agents Chemother **53:**202–209. http://dx.doi.org/10.1128/AAC.01074-08.

40. **Furuta Y, Takahashi K, Kuno-Maekawa M, Sangawa H, Uehara S, Kozaki K, Nomura N, Egawa H, Shiraki K.** 2005. Mechanism of action of T-705 against influenza virus. Antimicrob Agents Chemother **49:**981–986. http://dx.doi.org/10.1128/AAC.49.3.981-986.2005.
41. **Jin Z, Smith LK, Rajwanshi VK, Kim B, Deval J.** 2013. The ambiguous base-pairing and high substrate efficiency of T-705 (ravipiravir) ribofuranosyl 5′-triphosphate towards influenza A virus polymerase. PLoS One **8:**e68347. http://dx.doi.org/10.1371/journal.pone.0068347.
42. **Yuan S, Li G, Wang Y, Gao Q, Wang Y, Cui R, Altmeyer R, Zou G.** 2016. Identification of positively charged residues in enterovirus 71 capsid protein VP1 essential for production of infectious particles. J Virol **90:**741–752. http://dx.doi.org/10.1128/JVI.02482-15.
43. **Prichard MN, Shipman C, Jr.** 1990. A three-dimensional model to analyze drug-drug interactions. Antiviral Res **14:**181–205. http://dx.doi.org/10.1016/0166-3542(90)90001-N.
44. **Chou TC.** 2010. Drug combination studies and their synergy quantification using the Chou-Talalay method. Cancer Res **70:**440–446. http://dx.doi.org/10.1158/0008-5472.CAN-09-1947.
45. **Wu Y, Lou Z, Miao Y, Yu Y, Dong H, Peng W, Bartlam M, Li X, Rao Z.** 2010. Structures of EV71 RNA-dependent RNA polymerase in complex with substrate and analogue provide a drug target against the hand-foot-and-mouth disease pandemic in China. Protein Cell **1:**491–500. http://dx.doi.org/10.1007/s13238-010-0061-7.
46. **Hansen JL, Long AM, Schultz SC.** 1997. Structure of the RNA-dependent RNA polymerase of poliovirus. Structure **5:**1109–1122. http://dx.doi.org/10.1016/S0969-2126(97)00261-X.
47. **Kok CC, McMinn PC.** 2009. Picornavirus RNA-dependent RNA polymerase. Int J Biochem Cell Biol **41:**498–502. http://dx.doi.org/10.1016/j.biocel.2008.03.019.
48. **Thibaut HJ, Leyssen P, Puerstinger G, Muigg A, Neyts J, De Palma AM.** 2011. Towards the design of combination therapy for the treatment of enterovirus infections. Antiviral Res **90:**213–217. http://dx.doi.org/10.1016/j.antiviral.2011.03.187.
49. **Hung HC, Wang HC, Shih SR, Teng IF, Tseng CP, Hsu JT.** 2011. Synergistic inhibition of enterovirus 71 replication by interferon and rupintrivir. J Infect Dis **203:**1784–1790. http://dx.doi.org/10.1093/infdis/jir174.
50. **Arita M, Kojima H, Nagano T, Okabe T, Wakita T, Shimizu H.** 2013. Oxysterol-binding protein family I is the target of minor enviroxime-like compounds. J Virol **87:**4252–4260. http://dx.doi.org/10.1128/JVI.03546-12.
51. **Thompson AA, Peersen OB.** 2004. Structural basis for proteolysis-dependent activation of the poliovirus RNA-dependent RNA polymerase. EMBO J **23:**3462–3471. http://dx.doi.org/10.1038/sj.emboj.7600357.